Journal of Information Systems Engineering and Management
2025, 10(28s)
e-ISSN: 2468-4376
https://www.jisem-journal.com/

Research Article

Parametric Optimization of Ss316l on Selective Laser Melting for Enhanced Biocompatibility

S. Kirthana [1*], Dr. Sriram Venkatesh [2], Dr. T. Ramamohan Rao [3]
[1] *Phd Scholar, Department of Mechanical Engineering, University College of Engineering (A), Osmania University, Hyderabad, India. Email: kirthana6831@gmail.com*
[2] *Senior Professor, Department of Mechanical Engineering, University College of Engineering (A), Osmania University, Hyderabad, India*
[3] *Professor and HOD, Department of Mechanical Engineering, Vasavi College of Engineering, Hyderabad, India*
**Corresponding Author: S. Kirthana*

ARTICLE INFO

Received: 30 Dec 2024

Revised: 05 Feb 2025

Accepted: 25 Feb 2025

ABSTRACT

The Selective Laser Melting technique is widely employed in the production of complexly shaped end products for a range of industries, including biomedical, aerospace, automotive, and defence. SLM is a complicated manufacturing process since a lot of factors influence the characteristics of the items that are printed using it. The SLM printing of fully dense parts is becoming more and more popular for various high-end applications. Because of their biocompatibility following implantation, titanium alloy and stainless steel alloy are the materials most frequently used in the fabrication of implants. The primary objective of this study is the parametric optimization of the SS316L alloy manufacturing process on the DMP Flex 350, utilizing SLM as a 3D printing technique. Response surface methodology (RSM), an optimization technique, and a genetic algorithm were employed to determine the optimal laser power, scan speed, and hatching distance in order to produce samples with the highest potential porosity and compressive strength.

Keywords: Selective Laser Melting, SS316L alloy, Response surface Methodology, genetic algorithm.

INTRODUCTION

The tooling, automotive, medical, aerospace, and construction industries are among the areas seeing a rise in the use of metallic additive manufacturing. Figure 1.1 illustrates the six categories into which metal additive manufacturing can be further subdivided [1] and the proportion of industrial adoption by 2020. This image illustrates how the VAT photopolymerization process uses composites of photopolymer and metal particles rather than directly producing metal components. Based on this data, it is possible to draw the conclusion that the powder bed fusion metal AM technique is extensively utilized for the direct fabrication of metal parts across a variety of sectors, and that a deeper comprehension of these processes is necessary for a range of applications.

A layer of metal powder bed is utilized in the Powder Bed Fusion (PBF) procedure, wherein certain regions are melted or fused in accordance with the part's 3D model. PBF is primarily divided into two categories: laser and electron beam, depending on the energy source. Two popular PBF procedures that use laser and electron beam energy sources, respectively, are Selective Laser Melting (SLM) and Electron Beam Melting (EBM). Bhavar et al [2]. provided the main characteristics that distinguished the two PBF procedures. It may be concluded that SLM controls a great deal of the minimum feature sizes and geometric tolerances, even with EBM's rapid build speeds. Therefore, it would be simple to create intricately detailed parts with complex shape using the SLM technique.

SLM has the potential to be used to print complicated shaped parts with optimized design and reduced weight, based on the benefits of AM techniques. Any component's weight reduction strategy starts during the design stage.

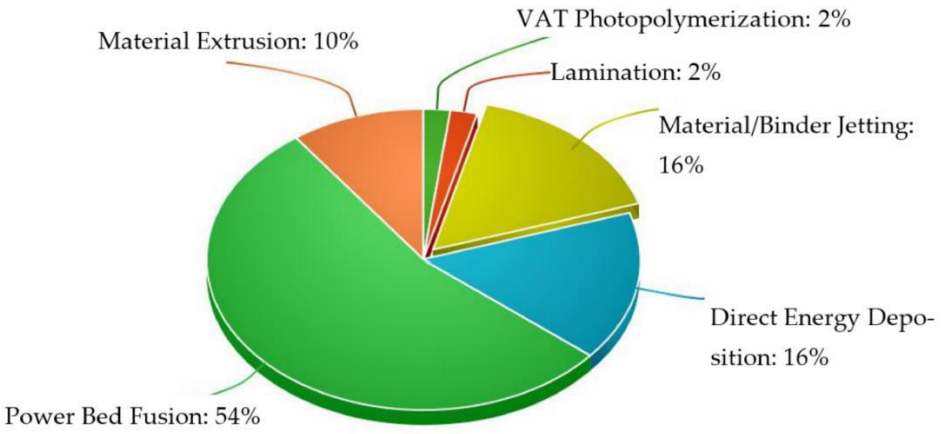

Fig 1.1 : A summary of the applications of additive manufacturing for metal in 2020

There is a lack of effort in suggesting new parameters that can accurately predict the density of parts using input parameters, even though a significant amount of research in additive manufacturing is dedicated to optimizing the relative density of metal printed parts through the adjustment of various process parameters. Energy density is a frequently used parameter in SLM process optimization to achieve a high relative density. This parameter includes a number of SLM parameters, including laser power, scan speed, hatch distance, and layer thickness, but it ignores the scan strategy and build orientation. Energy density can be expressed as follows [3]:

$$Energy\ density = \frac{LP}{SS*hs*lt} \quad (1)$$

Where LP is the power of the laser chosen, SS is the applied scan speed, HS is the given hatch spacing and lt is the thickness of each layer.

Researchers utilized this function to establish a connection between the density of SLM samples and the heat input, enabling the production of fully solid components. However, their common goal was to discover an optimal energy density level that corresponded to a low porosity content [4]. However, a number of research recommended using statistical analysis through the use of design of experiments (DoE) methods including the Analysis of Variance (ANOVA) and the Response Surface Method. The Central Composite Design (CCD) is widely acknowledged as a highly favored RSM design. The letter "k" represents the total number of components taken into account by this design. Included in the design are the two-level factorial, face points (sometimes called axial points), and center points (also called cube points). The statistical parameter known as α is utilized to regulate the axial points. Each factor in Central Composite Design is adjusted over 5 levels (-α, -1, 0, 1, and α) [5-6]. These methods were effectively used to examine how process variables, including scan speed, power of the laser and hatch spacing, affected the surface quality and percentage of porosity that were produced during the Selective Laser Sintering of SS316L alloy.

EXPERIMENTAL METHOD

Materials:

A material with many applications and versatility, stainless steel is prized for its exceptional strength and resistance to corrosion. The main constituents of this austenitic stainless steel are molybdenum, nickel, and chromium. This steel grade is highly sought after by various industries due to its exceptional combination of properties. It finds extensive applications in manufacturing, construction, food processing, and medical equipment. Due to its exceptional corrosion resistance, Type 316 is suitable for demanding environments such as chemical and maritime applications. 316 stainless steel typically consists of 69% iron, 16–18% chromium, 10–14% nickel, 2-3% molybdenum, 0.08% carbon, and traces of other elements.

Utilizing Response Surface Methodology to Conduct Design of Experiment (DOE):

The goal of this study's RSM experiment design was to create an experimental plan with the fewest number of trials achievable. Using analysis of variance (ANOVA), we were able to isolate critical parameters, establish a relationship between the input and output parameters, and then find the ideal parameter configuration to accomplish the target

function.[7] Equation 2 demonstrates the utilization of a second order polynomial equation to represent the response surface "Y".

$$Y = c_o + \sum c_i x_i + \sum c_{ii} x^2 + \sum c_{ij} x_i x_j \quad (2)$$

where xi denotes the input parameters of the factor. Process parameter main and secondary effects are represented by the model coefficients, which are c0, ci, cii, and cij. The constant coefficients are determined through the application of the least squares method. Using Design-Expert Software, the experiment's design was employed.

The following protocol was used in this study:

1. Establishing the boundary limits for each of the crucial process parameters.

2. Selecting the reaction that is generated.

3. Developing the matrix for the experimental design.

4. Carrying out the trials in accordance with step3 and noting down the resulting reaction.

5. To develop a mathematical model for connecting responses with input parameters.

6. Use Genetic algorithm to improve response efficiency.

In the current study, three elements were considered: hatch spacing, scan speed, and laser power. For this study, the value of α was set at two in order to evenly adjust each element across five levels. The quantities of each factor in this study are presented in Table 1. Here, α and -α represent the maximum and minimum levels of each factor, respectively [8,9]. Additionally, three center points were considered. The experimental error is evident in the use of the data points. Table 2 clearly shows that this resulted in the discovery of 14 different combinations for testing. Measurements were taken of various factors such as percentage of porosity, surface roughness, modulus of elasticity and Ultimate compressive strength (UCS) to gain a deeper understanding of the quality features of the produced samples.

Table1: Building parameters and their values for CCD

Parameter	Units	Levels chosen				
		- α	-1	0	1	α
LP	Watt	123	130	140	150	157
SS	mm/s	1164	1300	1500	1700	1836
HS	µm	26	40	60	80	94

Sample build and characterization:

The DMP Flex 350 was used to produce SLM components. Layer thickness of 30µm was chosen for building the specimen . Every step of the procedure was done in an argon environment with less than 0.1% oxygen. A circular coupon of 5 mm in diameter and 10 mm in height was created for every parametric condition.

Using a surface profilometer (Taylor Hobson Form Talysurf 120L), the surface roughness of the manufactured coupons was determined. In this work, the average surface roughness (R_a) served as the primary expression for the parts' surface quality. For every sample, two measurements were taken at the top surface and two at the side surfaces. The R_a was calculated across a 5mm diameter. Each sample's surface roughness was thought to be expressed by the average value of all the surface roughness values taken[10].

The samples were subjected to standard mechanical grinding and polishing using Silicon Carbide paper to achieve a 0.1 µm finish, which was necessary for microscopic analysis[11]. An optical microscope, specifically the Zeiss Gemini1 model, was utilized to examine polished surfaces. The microscope was installed with AV 4 image analysis software to aid in the study. For every sample, eight frames measuring 800 µm by 600 µm were taken, and ImageJ image analysis software was used to calculate the area fraction of the pores. [12]. The compression tests were conducted using a universal testing device, with a constant loading speed of 3 mm/min[13]. UCS and modulus of elasticity for each

specimen were determined by analyzing the stress-strain curves that emerged from the compression test. The investigation's 14 parametric conditions and their accompanying quality attributes are displayed in Table2.

Table 2: Test Responses for SS316L Alloy Samples

Run	A:Laser Power (W)	B:Scan Speed (mm/sec)	C:Hatching Space (µm)	Surface Roughness	Percentage of Porosity	Modulus of Elasticity (GPa)	UCS (MPa)
1	123	1500	60	11.62	20.93	25.27	454.1
2	130	1300	40	21.84	15.48	32.55	690.4
3	130	1300	80	17.53	6.19	65.11	1505.4
4	140	1836	60	18.49	10.81	48	1028
5	150	1300	40	18.61	26.33	18.32	358.1
6	140	1500	26	13.91	3.84	76.18	1614.3
7	150	1700	40	13.77	5.29	68.13	1537
8	157	1500	60	21.83	3.53	72.78	1385.4
9	140	1164	60	16.65	8.55	55.68	1147.3
10	140	1500	94	16.44	23.99	22.01	431.04
11	150	1300	80	10.6	4.76	67.63	1510.0
12	130	1700	40	16.08	8.7	50.13	1118.68
13	130	1700	80	16.08	22.6	22.83	394
14	150	1700	80	18.01	4.02	60.38	1238.7

RESULTS AND DISCUSSIONS

Table 2 displays the measured values for UCS, percentage of induced porosity, surface roughness, and Modulus of Elasticity in addition to the parametric combinations.

Analysis of Variance Results:

As a statistical metric, R^2 (or least square fitting) describes how well the model fits the data. Surface roughness (with an R2 value of 92%) and modulus of elasticity (with an R^2 value of 87%) both fit linear models according to the RSM method. Furthermore, the content of porosity can be accurately represented by a quadratic model, which has a high R^2 value of 98%. On the other hand, the UCS (unconfined compressive strength) is best described by a two-factor interaction model, which also has a respectable R^2 value of 95%. The surface roughness, modulus of elasticity, porosity, and UCS plots for the SS316L were compared and analyzed are shown in Figures 3.1 (a)–(d). The data points on each graph demonstrate that the actual values are always distributed closely around the line. As a result, it's possible that all of the models faithfully represented the relationship between the process parameters and the answer types studied here[14]. The general empirical model can be defined using Equation 3. Functions of laser power (LP), scan speed (SS), and hatch spacing (HS) are used to describe the four models.

$$\text{Response} = c_o + c_1(LP) + c_2(SS) + c_3(hs) + c_4(LP*SS) +$$

$$c_5(LP*hs) + c_6(SS*HS) + c_7(LP)^2 + c_8(SS)^2 + c_9(HS)^2 \quad (3)$$

The model coefficients, denoted as c1, c2, ..., c9, depend on the primary and secondary impacts of the process parameters. The coefficient c0 represents the average response. The coefficients for the quality attributes are displayed in Table 3. The study analyzed the responses and process parameters. Equation 3 can be utilized to establish the comprehensive empirical model, which can be expressed as functions of LP, SS and HS for the four models.

Table 3. RSM coefficients for the four models for SS316L Alloy

Model Coefficient	Surface roughness	Porosity	Modulus of Elasticity	UCS
c0	245.91	7.05	49.71	1153.43
c1	+2.87	-2.16	-0.5	176.87
c2	-0.41	4.95	-12.70	-295.06
c3	-0.26	4.36	202.52	-275.73
c4	0	-0.99	0	25.59
c5	0	-0.41	0	-61.12
c6	0	3.38	0	-187.97
c7	0	0.29	0	0
c8	0	1.51	0	0
c9	0	1.13	0	0

In statistical significance testing, the value of p reflects the probability of obtaining a test statistic as extreme as the observed one, assuming the null hypothesis that parameters have no significant influence is true. Given a probability value below the predetermined significance level of 0.05 (95% confidence level), the null hypothesis is rejected[15]. Accordingly, a model parameter is deemed significant if its p-value is less than 0.05. The p-values for the SS316L alloy's parameters and interactions are shown in Table 4. Based on the analysis of variance results, the laser power was found to be the most relevant parameter influencing surface roughness across the range of parameters examined in this study. On the other hand, scan speed, hatch spacing, and laser power were the most important elements influencing modulus of elasticity. In the end, the three process factors, along with the synergy between scan speed and hatch spacing, greatly affected the percentage of porosity and UCS.

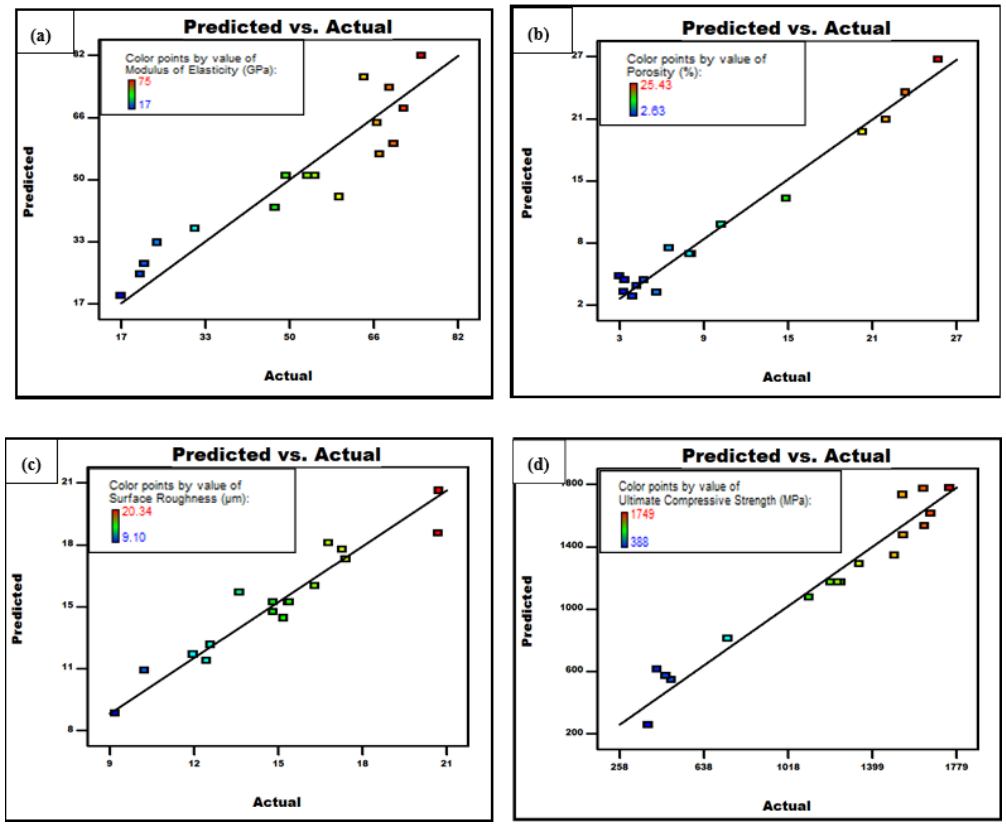

Fig 3.1. Comparing predicted and actual data for various properties of SS316L part, (a) Elasticity Modulus, (b) percentage of porosity induced, (c) surface roughness and (d) Ultimate compressive strength

Table 4: Probability values for the analysis of variance of each parameter for SS316L

Model Parameter	Probability value			
	Surface roughness	Percentage of Porosity	Modulus of Elasticity	UCS
LP	**< 0.00098***	**0.00158**	**0.0051**	**0.00054**
SS	0.1205	**< 0.00022**	**< 0.000932**	**< 0.00092**
HS	0.31446	**< 0.000873**	**< 0.00091**	**< 0.000934**
LP*SS	-	0.235	-	0.6045
LP*HS	-	0.5693	-	0.2183
SS*HS	-	**0.00089**	-	**0.00342**
LP2	-	0.4786	-	-
SS^2	-	0.0059	-	-
HS^2	-	0.0197	-	-

Surface Roughness Analysis:

As previously noted, a linear model depicts the relationship between the two variables and the power of the laser alone had a large impact on surface roughness. The impact of laser power on surface roughness for SS316L alloys is displayed in Fig. 3.2. It is evident that a considerable decrease in the R_a value from 21 to 18µm occurred when the laser power was increased from 130W to 150W while maintaining a constant scan speed and hatch spacing of 1300 mm/s and 40µm, respectively. This implies that the top surface and side surface of the printed pieces might both be considerably smoothed out by increasing the laser power. A flatter melt pool and better surface quality are the results of higher recoil pressures, which are produced by more powerful laser[16].

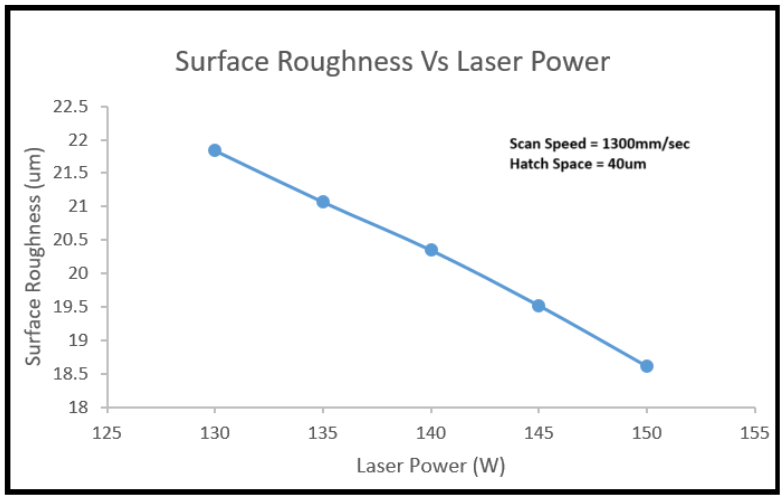

Fig 3.2 Analysis of the surface roughness as a function of laser power for SS316L

Porosity Analysis:

The use of high energy causes capillary forces and surface tension to close holes, increasing the density of SLM samples. Additionally, obtaining continuous tracks is ensured by low scan speed. Due to the increased overlapping area of nearby scanning lines, a short hatching spacing would result in the powder between scanning lines melting entirely. Due to the succeeding pool of melting accumulating on the previously formed layer and the solidified scanning lines, the scanning line would gradually transition from melt to solid[17]. As the distance between hatches increases, the impact of scan speed on porosity development also increases. The SS316L alloy exhibited the same behavioural pattern, as seen in Fig. 3.3(a) through (c).

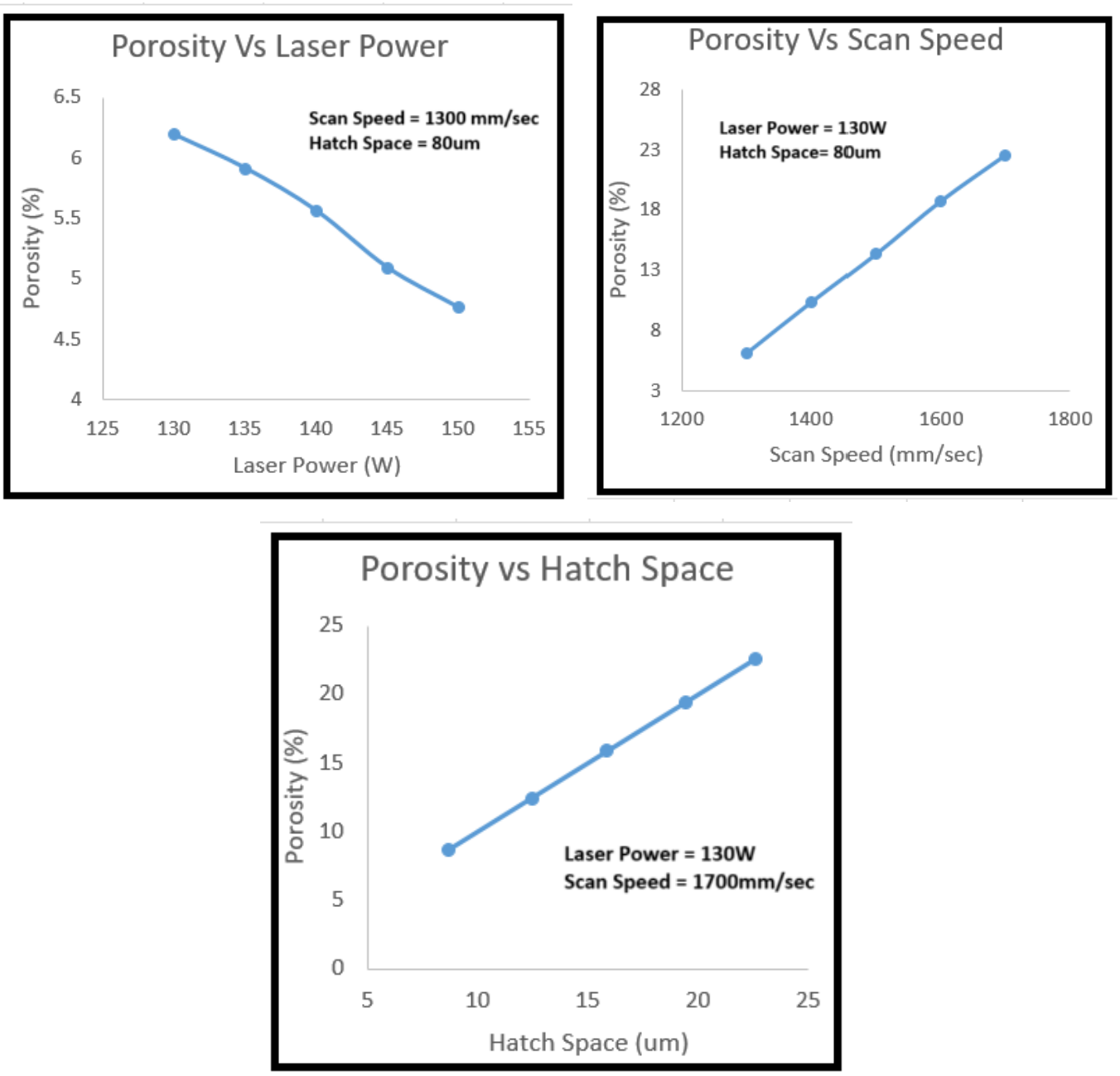

Fig 3.3 Impact of various parameters on porosity.

Microphotographs of samples 9 and 2, respectively, for the SS316L alloy are displayed in Figs. 5.20 and 5.21 (See Table 2).Samples 9 and 2 of SS316L had porosity contents of 8.55% and 15.48%, respectively. When using a slower scanning speed and higher laser power (sample 9), it was observed that the material displayed a notable increase in density, as illustrated in Figure 3.4. Alternatively, when the laser power is low and the scan speed is fast, the energy may not be sufficient to fully solidify the powder. This leads to the formation of structures with pores, as shown in Figure 3.5. Because of its low elastic modulus, an implant made of SS alloy with a structure like sample 2 is advised for use in biomedical applications. Furthermore, the pores will facilitate the easy growth and integration of tissues with the implant.

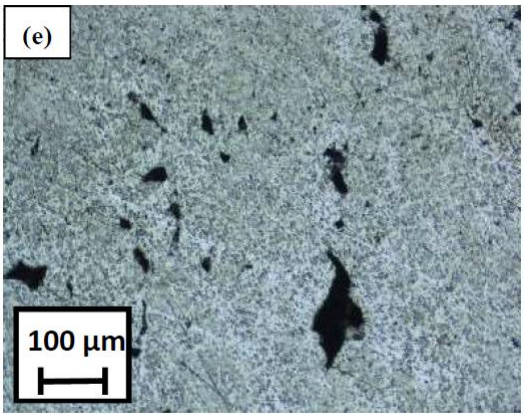

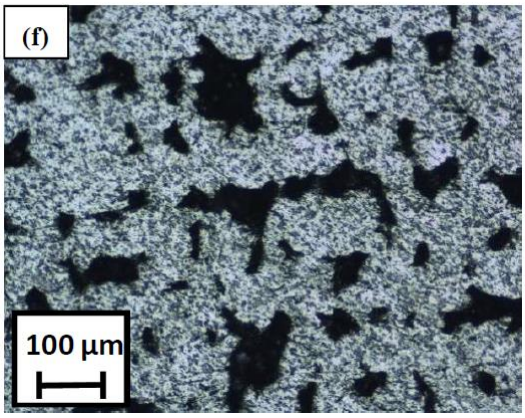

Fig.3.4 Micrograph of sample9 of SS Alloy Fig3.5 Micrograph of sample 2 of SS Alloy

Analysis on Elastic Modulus:

As seen in Fig. 3.6(a) to (c) for SS316L Alloy, it was discovered that all three process factors had a considerable impact on the elastic modulus of the manufactured samples. The three parameters were found to be linear functions of elastic modulus. An increase in laser power was shown to increase the modulus of elasticity. Reducing the scan speed and/or hatch spacing could have the same effect on characteristics.

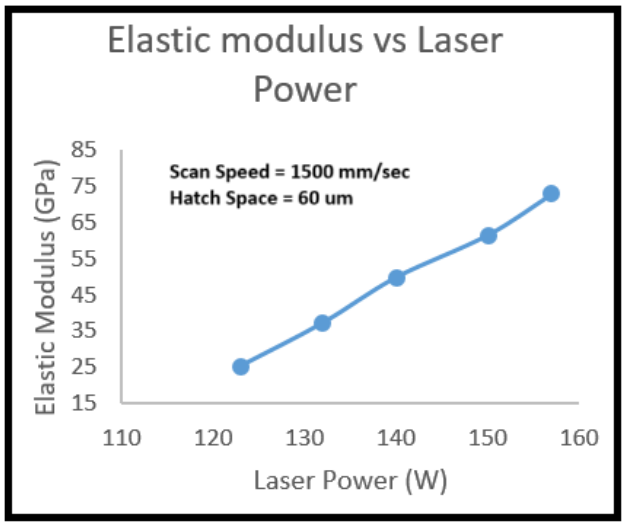

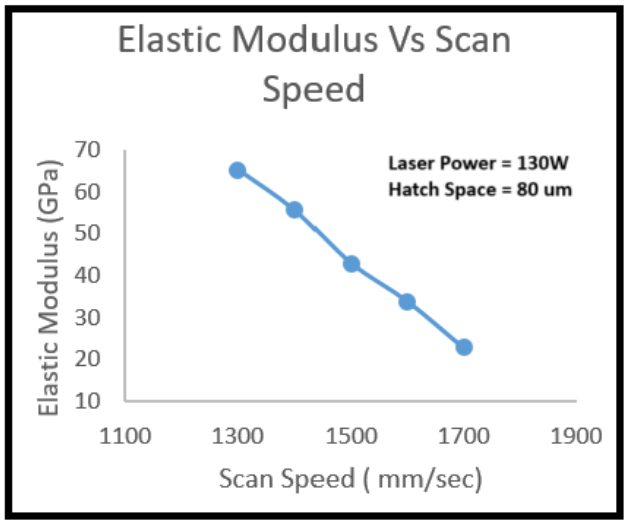

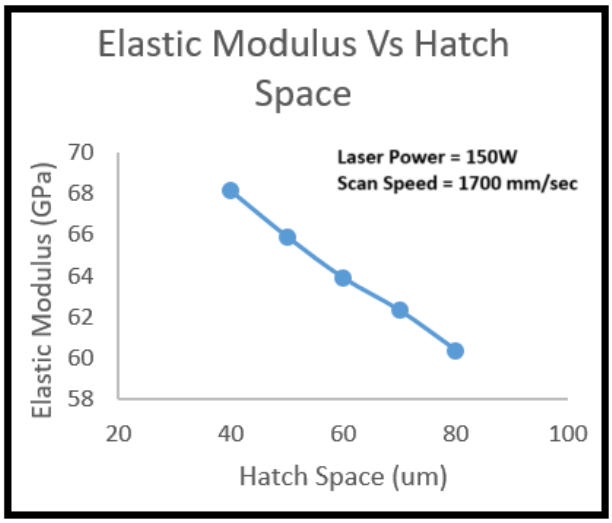

Fig 3.6. Impact of various factors on modulus of elasticity

Analysis of Ultimate Compressive strength:

Like the elastic modulus, the model predicted that the UCS would be directly related to laser power and inversely related to scan speed and hatch spacing (See Figs 3.7(a), (b) and (c)). The UCS was also shown to be significantly affected by the interaction between scan speed and hatch spacing. Increasing the hatch spacing while maintaining the same laser power resulted in a steeper slope for the scan speed versus UCS relationship[18]. Nonetheless, it was proposed that UCS be depicted as a 2FI model of the parameters involved in the SLM process.

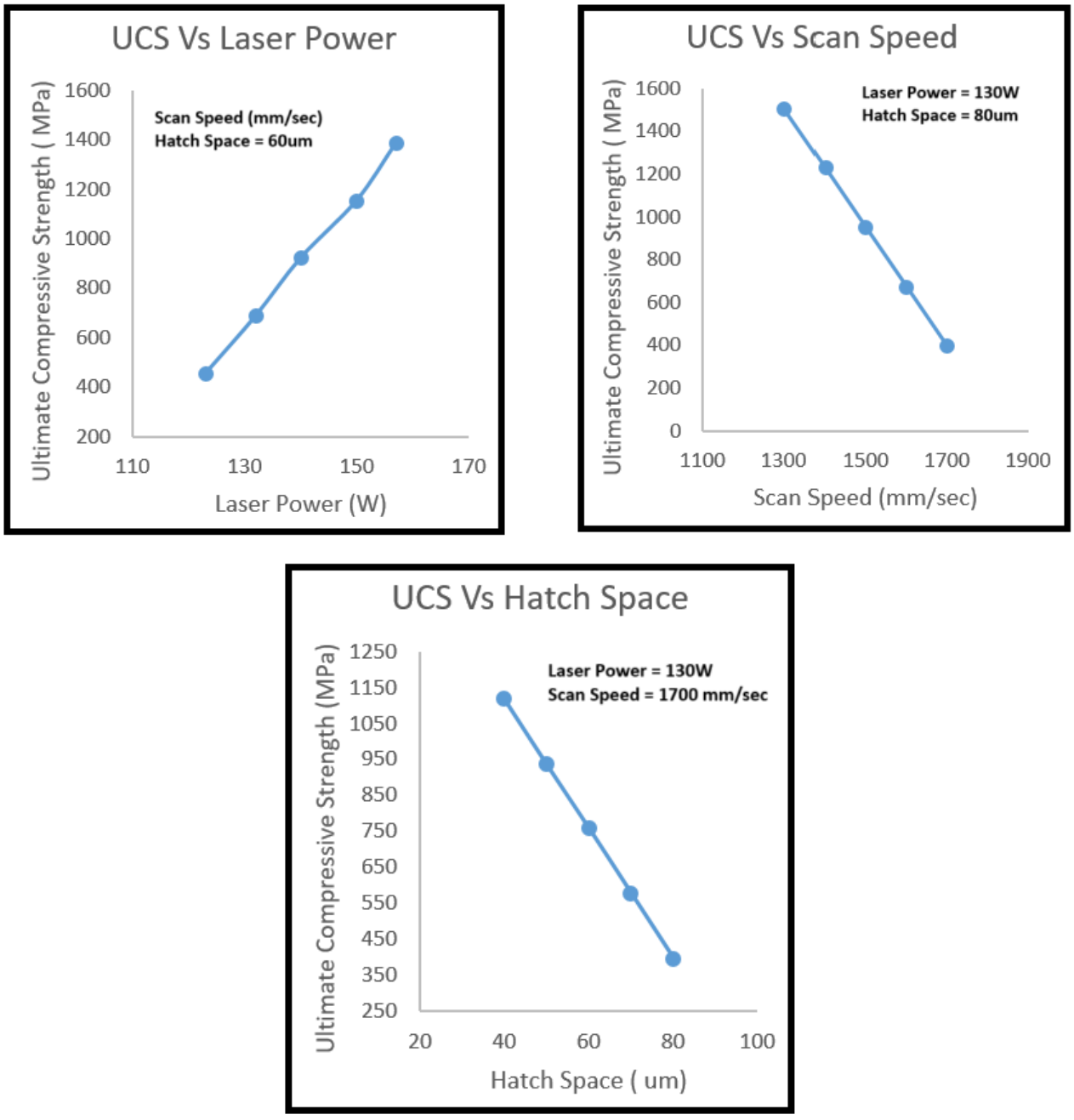

Fig3.7 Impact various factors on Ultimate compressive strength

3.6 Explaining the formation of porosity by analysing the energy density:

If the energy density is insufficient to achieve complete melting and even distribution of the powder, the final build may exhibit the formation of pores. There will be less melt pool and partial consolidation if the considered factors are increased. Consequently, when the powder particles solidify, the spaces between them get trapped under the hatch lines[19]. This leads to an increase in the porosity content, which in turn reduces the overall density of the SLM part. This is a crucial requirement for implants. With the enhanced consolidation of the metal powder, the porosity content

steadily decreases as the energy density rises, ultimately reaching a minimum value between 90 J/mm^3 and 130 J/mm^3. Nevertheless, the porosity content scatters up to 180 J/mm^3 when the energy density increases further. Other defects, including keyhole development (caused by vaporization) within the SLM portion, may also occur in this area, raising the porosity level overall.

Optimization towards medical applications:

To determine the ideal processing parameter setting required for SLM of an SS316L component with properties appropriate for orthopaedic surgery, an optimization research was conducted. The goal function was to get the maximum matching UCS and porosity percentage while obtaining a modulus of elasticity in the limits of 10 to 30 GPa and a surface roughness between 1 μm and 10 μm[20]. The Design-Expert program examined the experimental data, and the genetic algorithm was utilized to forecast the process parameters that meet the objective function[21]. Simultaneous solutions were found for the response equations that describe the responses considered in terms of the important process parameters. A 1400 mm/s scan speed, a 125 W laser output, and an 88 μm hatch spacing would be the model's recommended optimal values for the process parameters for SS316L. An energy density of 33.82 J/mm^3 is corresponding to this. For an SLM part, the estimated surface roughness, porosity, modulus of elasticity, and UCS at these process parameter values would be 7.78 μm, 15.42%,29 GPa, and 445 MPa, in that order.

CONCLUSIONS

The effects of the SLM process parameters on the quality attributes of SS316L SLM parts were examined. The most important factors were determined and an experimental plan was created using the RSM and ANOVA. The best process parameter setting to yield parts with qualities appropriate for orthopedic structure was determined using the generic method. The findings acquired allow for the conclusion of the following points:

1. When the laser power was increased, a noticeable decrease in surface roughness was observed for the SLM component. It is probable that the melt pool flattened during the process, leading to a decrease in surface roughness and the elimination of balling. These changes are anticipated to enhance the overall quality of the side surfaces of the SLM parts.
2. Through improved consolidation of the metallic powder, adjustments such as increasing the laser power or reducing the scan speed and hatch spacing (within a certain range) resulted in a decrease in porosity level for the SLM part. As a result, the part's UCS and modulus of elasticity were increased. In addition, the mechanical properties of an SLM component demonstrated a significant relationship with the amount of pores present. This indicates that the porosity level of the SLM part can be precisely adjusted to alter its characteristics.
3. The recommended laser power for SS316L is 125 W, with a scan speed of 1400 mm/s and a hatch spacing of 88 μm. The energy density is 33.82 J/mm^3. Based on the given process parameter values, the expected values for the surface roughness, porosity, modulus of elasticity, and UCS at these process parameter values would be 7.78 μm, 15.42%,29 GPa, and 445 MPa.

REFERENCES

[1] Stavropoulos, P.; Foteinopoulos, P.; Papacharalampopoulos, A.; Bikas, H. Addressing the challenges for the industrial application of additive manufacturing: Towards a hybrid solution. (2018) Int. J. Light. Mater. Manuf., 1, 157–168.

[2] Bhavar, V., Kattire, P., Patil, V., Khot, S., Gujar, K., and Singh, R.,(2017), A review on powder bed fusion technology of metal additive manufacturing, Additive manufacturing handbook, CRC Press. p. 251-253.

[3] Read N, Wang W, Essa K, Attallah MM (2015) Selective laser melting of AlSi10Mg alloy : Process optimisation and mechanical properties development. Materials and Design 65:417-424.

[4] Olakanmi EO, Cochrane RF, Dalgarno KW (2011) Densification mechanism and microstructural evolution in selective laser sintering of Al–12Si powders. Journal of Materials Processing Technology 211 (1):113-121.

[5] Song B, Dong S, Zhang B, Liao H, Coddet C (2012) Effects of processing parameters on microstructure and mechanical property of selective laser melted Ti6Al4V. Materials & Design 35:120-125.

[6] El-Sayed MA (2018) Parametric analysis of SLM process for fabricating 316L stainless steel samples by response surface method, Journal of engineering technology, emerging trends in engineering and technology.

[7] Vaithilingam, J., Prina, E., Goodridge, R.D., Hague, R.J., Edmondson, S., Rose, F.R. and Christie, S.D. (2016), "Surface chemistry of Ti6Al4V components fabricated using selective laser melting for biomedical applications", Materials Science and Engineering. C, Materials for Biological Applications, Vol. 67, pp. 294-303.
[8] Elsayed, M., Ghazy, M., Youssef, Y., & Essa, K. (2018). Optimization of SLM process parameters for Ti6Al4V medical implants. Rapid Prototyping Journal.
[9] Alla, R.K., Ginjupalli, K., Upadhya, N., Shammas, M., Ravi, R.K. and Sekhar, R. (2011), "Surface roughness of implants: a review", Trends in Biomaterials and Artificial Organs, Vol. 25 No. 3, pp. 112-118.
[10] Read, N., Wang, W., Essa, K., & Attallah, M. M. (2015). Selective laser melting of AlSi10Mg alloy: Process optimisation and mechanical properties development. Materials & Design (1980-2015), 65, 417–424.
[11] Ribeiro, M. V., Moreira, M. R. V., & Ferreira, J. R. (2003). Optimization of titanium alloy (6Al–4V) machining. Journal of Materials Processing Technology, 143-144, 458–463.
[12] Deepak Doreswamy, D.sai Shreyas, Subraya Krishna Bhat, RajathRao, (2022), Optimization of material removal rate and surface characterization of wire electric discharge machined Ti-6Al-4V alloy by response surface method, Journal of manufacturing review, volume 9,15-25.
[13] Sahu, N. K., & Andhare, A. B. (2015). Optimization of Surface Roughness in Turning of Ti-6Al-4V Using Response Surface Methodology and TLBO. Volume 4: 20th Design for Manufacturing and the Life Cycle Conference; 9th International Conference on Micro- and Nanosystems.
[14] Baris Sener, Oktay CAVusoglu, Celattin yuce, Effects of process paramters on surface quality and mechanical performance of 316L stainless steel produced by selective laser melting, Optik, volume 287, 2023, 171050.
[15] Mohammadamin Bakhtiarian, Hamid Omidvar, The effects of SLM process parameters on the relative density and hardness of austenitic stainless steel 316L, Journal of materials research and technology, volume 29, 2024, pg 1616-1629.
[16] Gong G, Ye J, Chi Y, Zhao Z, Wang Z, Xia G, et al. Research status of laser additive manufacturing for metal: a review. J Mater Res Technol 2021;15:855–84.
[17] Park S-H, Son S-J, Lee S-B, Yu J-H, Ahn S-J, Choi Y-S. Surface machining effect on material behavior of additive manufactured SUS 316L. J Mater Res Technol 2021; 13:38–47.
[18] Bansal GK, Chandan AK, Srivastava VC, Krishna KG, Das G, Rajkumar S, et al. Studies on tensile behaviour of selective laser melted 316l stainless steel using SEM straining stage. Trans Indian Natl Acad Eng 2021;6:1005–15.
[19] Tucho WM, Lysne VH, Austbø H, Sjolyst-Kverneland A, Hansen V. Investigation of effects of process parameters on microstructure and hardness of SLM manufactured SS316L. J Alloys Compd 2018;740:910–25.
[20] Tolosa I, Garciandía F, Zubiri F, Zapirain F, Esnaola A. Study of mechanical properties of AISI 316 stainless steel processed by "selective laser melting". following different manufacturing strategies. Int J Adv Manuf Technol 2010;51: 639–47.
[21] Huang M, Zhang Z, Chen P. Effect of selective laser melting process parameters on microstructure and mechanical properties of 316L stainless steel helical microdiameter spring. Int J Adv Manuf Technol 2019;104:2117–31.